Published by Associazione Teriologica Italiana
Volume 33 (1): 80–91, 2022

Hystrix, the Italian Journal of Mammalogy

Available online at:

http://www.italian-journal-of-mammalogy.it
doi:10.4404/hystrix-00478-2021

Research Article

Physiological response of a wild rodent to experimental manipulations in its natural environment using infrared thermography

Yiannis G. Zevgolis*, Stylianos P. Zannetos, Triantaphyllos Akriotis

Biodiversity Conservation Laboratory, Department of Environment, University of the Aegean, 81100 Mytilene, Greece

Keywords:
rodents
Apodemus mystacinus
Stress-Induced Hyperthermia
Infrared Thermography
non-invasive methods
field methods

Article history:
Received: 4 August 2021
Accepted: 10 March 2022

Acknowledgements
We are very grateful to the Editor-in-Chief Dr Lucas A. Wauters as well as to Marina Morandini for their constructive comments, suggestions, and extensive editing of our original manuscript, greatly improving it. We would also like to thank K. Vlachopoulos for valuable discussions and help with the data analysis, G.D. Kokkoris for his effective guidance in statistical methods and G. Charea for her help during field work.
This research is carried out / funded in the context of the project "Study of acute and chronic physiological and behavioral response of small mammals to stressful stimuli, using non-invasive methods in field sampling conditions" (MIS 5048921) under the call for proposals "Supporting researchers with an emphasis on new researchers" (EDULLL 103). The project is co-financed by Greece and the European Union (European Social Fund- ESF) by the Operational Programme Human Resources Development, Education and Lifelong Learning 2014–2020.

Abstract

Heat loss from non-insulating body parts of rodents can be used as a proxy to Stress-Induced Hyperthermia (SIH) and can be detected via non-invasive methods, such as infrared thermography (IRT). Although IRT has been systematically used to detect SIH in captive or laboratory animals, very few studies have been performed in wild situations. We investigated the SIH in a wild rodent, the Eastern Broad-toothed Field Mouse *Apodemus mystacinus*, faced with novel stressors in its natural habitat, using IRT. We subjected live-trapped individuals to six consecutive experimental manipulations (Experimental Manipulations Phase - EMP), and then we temporarily transferred them to a wooden box to partly overcome the stressful challenges (Transitory Release Phase - TRP). We used the maximum eye temperature difference between the start of the EMP and the start of the TRP (ΔT_{SIH}) as the best estimate of SIH. Mean eye temperature during EMP differed significantly from that of TRP for each individual and the differences were similar when examined separately as to sex, trapping history, or breeding condition. Comparison of eye temperature time series for different trapping history groups showed a higher similarity of the response of first captures with 2nd and 3rd recaptures than of first captures with 1st recaptures, verified by a comparison of ΔT_{SIH} for these groups. Larger-sized first-captured individuals appeared less stressed by the experimental procedure than smaller-sized individuals. Overall, IRT appears to be a useful and feasible method for non-invasive monitoring of SIH.

Introduction

Recent developments in remote sensing have established the use of infrared thermography (IRT), a rapidly developing technique and potentially an important tool applied in various fields of Ecology (Still et al., 2019; Cilulko et al., 2013). IRT has been increasingly used for unobtrusive and contactless monitoring in animal studies (McCafferty, 2007). In recent years, IRT has been used to diagnose diseases (Mota-Rojas et al., 2021; Dunbar et al., 2009), to investigate thermoregulatory mechanisms (Briscoe et al., 2014; Tattersall and Cadena, 2010), to study animal behaviour (Mazur-Milecka, 2016; Horton et al., 2015), and it is also a valuable tool in the assessment of animal physiological stress (Travain and Valsecchi, 2021; Jerem et al., 2019).

Physiological stress in animals is frequently described as the set of adaptive physiological responses to an aversive extrinsic stimulus (a "stressor") which alters their homeostatic status (Dantzer et al., 2014; Romero, 2004). The stressor can be generated from a predictable (e.g., seasonal changes in food availability, physical condition or reproductive status) or (b) unpredictable environmental stimulus (e.g., risk of predation, captivity or handling) (Dantzer et al., 2014; Romero, 2004). Under acute stress, vertebrates display a generic physiological pattern for coping with difficult situations: the sympathetic-adrenal-medullary system and the hypothalamic-pituitary-adrenal axis are activated with the secretion of adrenalin, resulting in a patterned curdle-vascular response consisting of the increase of blood pressure, heart, respiratory, and metabolic rate, and blood glucose, fatty acid, amino acid and glucocorticoid levels (Smith and Vale, 2006; Sapolsky et al., 2000). Active vasodilatation in skeletal muscles and vasoconstriction in intestines, kidneys, and skin leads to a redistribution of blood flow from the visceral and cutaneous beds towards the vasculature of the skeletal muscles (Crestani, 2016; Mohammed et al., 2013, 2014; Blessing, 2003). These changes prepare the animal to promptly respond at the stressor either passively ("withdrawal" — Engel and Schmale, 1972), or actively ("fight or flight" — Steimer, 2011).

Abbreviations
The following abbreviations are used in this manuscript:
BW Body weight
CL Condylobasal length
EL Ear length
EMP Experimental Manipulations Phase
HBL Head and body length
HFL Hind foot length
IRT Infrared thermography
RB Recuperation box
SIH Stress-induced hyperthermia
TL Tail length
TRP Transitory Release Phase

Conceptualization, Y.G.Z., S.P.Z., T.A.; Methodology, Y.G.Z., S.P.Z., T.A.; Formal analysis, Y.G.Z.; Investigation, Y.G.Z. and S.P.Z.; Resources: Y.G.Z., S.P.Z., T.A.; Writing – original draft preparation, Y.G.Z.; Writing – review and editing, Y.G.Z. and T.A.; Visualization, Y.G.Z.; Supervision, T.A.

*Corresponding author
Email address: zevgolis@env.aegean.gr (Yiannis G. Zevgolis)

©2022 Associazione Teriologica Italiana

Physiological response of animals to stressful stimuli is also characterized by elevated core body temperature, a phenomenon named stress-induced hyperthermia (SIH) or emotional fever (Van Der Heyden et al., 1997; Cabanac and Briese, 1992; Briese and Cabanac, 1991). SIH is proportional to stressor intensity (Bouwknecht et al., 2007) and it is frequently associated with radiated heat loss from animals' thermoregulatory body parts (Nord and Folkow, 2019). SIH has been described in a variety of endothermic species including humans (Oka et al., 2013), laboratory animals (Schmelting et al., 2014), farm animals (Lees et al., 2020; Sanger et al., 2011), and wild mammals and birds (Bittencourt et al., 2015; Jerem et al., 2015; Careau et al., 2012). SIH appeared in response to a variety of stressors, such as cage change / cleaning (Rasmussen et al., 2011; Burn and Mason, 2008), exposure to a new environment (Amico et al., 2004), fear of predation (Rorick-Kehn et al., 2005), and handling (Nord and Folkow, 2019; Lewden et al., 2017; Olivas and Villagrá, 2013).

In rodents, mainly laboratory mice and rats, SIH usually involves an increase of the core body temperature by 0.5–1.5 °C (McGivern et al., 2009; Bouwknecht et al., 2007; Dallmann et al., 2006). Traditional methods of measuring animal core body temperature are mostly invasive as they require the use of thermocouples or thermistors, surgical implants, gastrointestinal devices, or passive transplants (McCafferty et al., 2015). An alternative non-invasive method for the assessment of stress is the determination of glucocorticoid concentration in urine, faeces or hair (Palme, 2019). Although this method may be useful for captive or laboratory animals, there are two potential problems when used in the field. First, the increase of glucocorticoid levels can also depend on other factors such as food ingestion, prey capture or mating opportunity (Thierry et al., 2013; Buwalda et al., 2012). Second, although it has been shown that time elapsed since a stressful event is an important factor influencing the level of glucocorticoids in faeces Dantzer et al. (2016); Möstl et al. (2005); Palme (2005), the time of production of faeces in trapped animals is usually not known. However, checking traps frequently can strongly reduce the time between defaecation and faeces collection, excluding any potential bias in the measurement of faecal glucocorticoid metabolites (Tranquillo et al., 2022). An additional difficulty in the case of small mammals is that the quantities may be not be sufficient for the analysis (Harper and Austad, 2000, 2001).

Small mammals achieve thermal homeostasis using "thermal windows", losing heat from specific parts of their body surface, to balance heat gain from metabolic processes (Šumbera et al., 2007). IRT can detect surface temperature changes in thermal windows, such as the eye area, resulting from blood flow changes and it can be a useful non-invasive tool for quantifying heat loss (Stewart et al., 2005). Measurement of maximum eye temperature is considered the most important non-invasive indicator for detecting physiological stress (Edgar et al., 2011; Stewart et al., 2007; Cook et al., 2005, 2001). In comparison with other thermal windows, eye temperature is closer to core body temperature due to a more constant blood supply and the absence of insulation (Ikkatai and Watanabe, 2015; McCafferty et al., 2015; Church et al., 2014). Maximum eye temperature has been used as an index for the detection of physiological responses related to stress in handling processes (Bartolome et al., 2019; Herborn et al., 2018; Schaefer et al., 2012) such as cattle castration (Stewart et al., 2010), horn-cutting in deer and cows (Stewart et al., 2009; Cook et al., 2005), and in handling trapped wild birds (Jerem et al., 2015; Møller, 2010). However, although IRT has been systematically used for this purpose in captive and laboratory animals, few studies have been carried out with animals in the wild (Jerem et al., 2019, 2015).

Our aim was to investigate the use of IRT in the study of physiological response of a wild rodent to novel stressors in its natural environment. We based our study on the Eastern Broad-toothed Field Mouse Apodemus mystacinus, a relatively common species in the NE Mediterranean region (Kryštufek and Vohralík, 2009, *pers. obs.*). We subjected live-trapped individuals to a standard field study handling procedure with concurrent recording of the eye temperature. We hypothesize that when a wild rodent being handled exhibits SIH, its eye temperature can be monitored non-invasively using IRT. We predict that mean eye temperature will be high but more variable while the animal is being handled and that eye temperature will subside and be more uniform when the animal is placed in dark and quiet conditions. Previous experience of trapping and handling may affect the stress response (Bosson et al., 2012; Fletcher and Boonstra, 2006; Long et al., 1990), thus, we predict that eye temperature fluctuation will show a greater similarity between first captures and 1st recaptures than of first captures with 2^{nd} or 3^{rd} recaptures and that a lower SIH is displayed in recaptured individuals due to habituation. Body size affects heat inertia (Phillips and Heath, 1995), however, we predict that the effect of body size on SIH is slight or non-existent in similar-sized mature conspecifics.

Materials and Methods

Study sites and species selection

The study site is in the island of Lesvos, in the north-eastern Aegean Sea, Greece. Lesvos has an area of 1632.8 km^2, with a Mediterranean climate (hot-dry summer, cool-wet winter). For our study we selected the most common and widespread species of rodent present in the island, the Eastern Broad-toothed Field Mouse (A*podemus mystacinus*), which can be found in areas characterized by tree — or shrub — cover and rocky terrain (Kryštufek and Vohralík, 2009, *pers. obs.*). Two sites with suitable habitat were selected in the central part of the island, 7 km apart, for the purpose of trapping.

Experimental manipulations of *A. mystacinus*

We trapped small mammals from 26 April to 26 May and from 24 September to 01 November 2020. In trapping and handling the animals we followed the guidelines of the American Society of Mammalogists (Sikes and Gannon, 2011); none of the captured individuals was injured or died during the experimental procedure. In each trapping period at each field site, we used 20 standard-sized collapsible live-traps (LFATDG, 7.6×8.9×22.9 cm, H.B. Sherman Traps Inc.) on five successive nights, followed by a week's break and a further five successive trapping nights. We activated traps thirty minutes after sunset and we inspected them every morning starting at first light and finishing by one hour after sunrise. We covered traps with bubble wrap and we introduced dry grass and pine needles to provide a warm environment, reducing thermoregulatory stress of captured individuals during the night.

We processed each individual in two phases (Fig. 1): the Experimental Manipulations Phase — EMP, and the Transitory Release Phase — TRP. The EMP started with the extraction of the animal from the trap, followed by six consecutive manipulations. Each manipulation consisted of appropriately positioning the animal in the hand and meas-

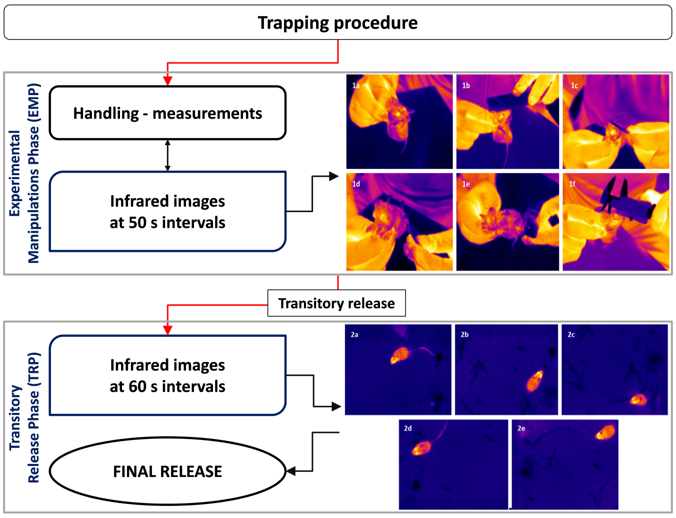

Figure 1 – Methodological procedure divided into two phases; (a) the EMP, experimental manipulations with simultaneous IR imaging, and (b) the TRP, IR images taken in the Recuperation Box (RB) before the final release of individuals. Each experimental manipulation is represented through the IR images 1a to 1f, while each IR image in the TRP (2a–2e) represents the per-minute state in the RB.

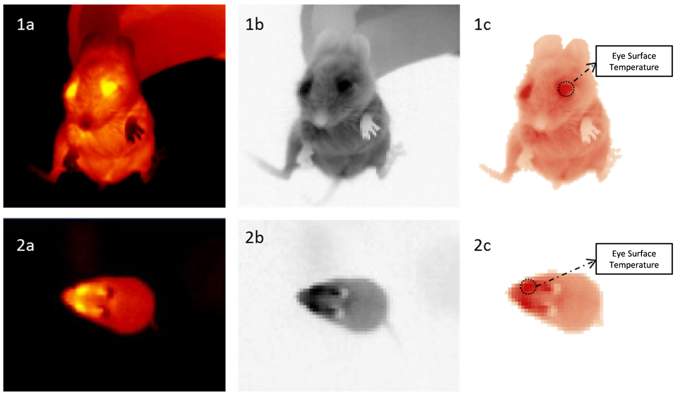

Figure 2 – Process of extracting eye surface temperature values of an *A. mystacinus* during the two phases; (a), (b) and (c) refer to the EMP while (d), (e) and (f) to the TRP. (a)/(d): Initial IR image after calibration; (b)/(e): Inverted greyscale IR image; (c)/(f): IR image enhancement and separation of the animal from its background.

uring a specific morphometric trait in the following standard order: body weight (BW), condylobasal length (CL), head and body length (HBL), hind foot length (HFL), tail length (TL), and ear length (EL). We additionally tagged first-captured individuals with unique ear tags (Style 1005-1, 100×2.36 mm, National Band and Tag Co., Newport, KY, USA). All experimental manipulations and measurements were performed by the same operator, to minimise measurement error.

The total duration of the experimental manipulations of EMP was five minutes (50 s per manipulation). At the end of this period, we transferred each animal into a dark wooden "recuperation box" (RB) (start of TRP). The RB had a 40×40 cm floor area, a height of 50 cm, and a cut-out at the centre of the roof to accommodate the thermal camera, for taking images of the floor area. Each animal stayed in the RB for five minutes, in absolute darkness, to partly overcome the stress of the previous procedure. Based on preliminary investigation in previous trials in 2019 (unpublished data), we selected a five-minute length of stay in the RB as the optimum compromise between the need for adequate time for the animal to come to a relatively calm state and the need to process and release all the trapped animals in the shortest possible time. Before each use, we placed fresh dry grass and leaves at the bottom of the RB. At the end of the TRP the animal was released through four 5×5 cm openings, one on each side of the RB, remotely opened with a simple string and pulley system.

Collection of infrared images

We photographed each individual using a handheld thermal camera (Testo 875-1i, Testo SE & Co. KGaA, Lenzkirch, Germany), with a thermal resolution of <0.08 °C and a thermal sensitivity of <50 mK. Resulting infrared (IR) images had a resolution of 160×120 pixels, during both the EMP and the TRP. In order to avoid (a) the effect of atmospheric composition (e.g. floating particles, soil dust, Minkina and Dudzik, 2009) and (b) temperature inaccuracies due to the entrance of solar radiation through the tree canopy, IRT was performed only on days with light wind and in the early morning hours. We positioned the thermal camera at the closest possible distance from the animals: 0.3 m during the EMP and 0.4 m during the TRP. We used a slightly longer distance for the TRP to minimise disturbance while ensuring a sufficient number of pixels of the animals' eye area for accurate surface temperature estimation (Tattersall, 2016; Faye et al., 2016; Tattersall and Cadena, 2010). In total, we collected a minimum of eleven IR images for each individual; six during the EMP (one per manipulation, at 50 s intervals) and five during the TRP (at 60 s intervals). We assured that both eyes were clearly visible in these pictures (Gjendal et al., 2018; Langford et al., 2010).

The thermal camera was calibrated using an emissivity coefficient (ε) of 0.95, a value considered suitable for the ocular surface of rodents (Vogel et al., 2016). Additional data required for calibration were obtained with a portable weather station and a solar radiation meter (Amprobe SOLAR-100).

Determination of Eye Surface Temperature

We initially processed the collected raw IR images using the TESTO IRSoft® software (v. 4.3). The region of interest (eye area) was separated from other objects in the background and manually bounded by a unique polygon (Fig. 2). Following image enhancement to improve contrast, we extracted the temperature values for all pixels within this polygon. We determined the maximum eye temperature (T_{max}) for each IR image by creating a histogram of the temperature values for each IR image and then averaging the values between μ+2σ and μ+3σ of each histogram. We, thus, obtained a single mean value as a representative statistical metric of Tmax. For each capture, we obtained six T_{max} values for EMP, one per manipulation (T_{BW}, T_{CL}, T_{HBL}, T_{HFL}, T_{TL}, T_{EL}), and five T_{max} values for TRP at 60 s intervals (T_{60}, T_{120}, T_{180}, T_{240}, T_{300}). We further derived a set of thermal variables related to T_{max} central tendency and variability measures: (a) mean T_{EMP} and mean T_{TRP} ($T_{meanEMP}$, $T_{meanTRP}$) for all EMP or TRP measurements of each individual respectively, and (b) the range ($T_{rangeEMP}$, $T_{rangeTRP}$) of all EMP and TRP measurements of each individual respectively. We also calculated an additional variable describing each individual's response to experimental manipulations as the difference in T_{max} between the two phases ($\Delta T_{SIH} = T_{BW} - T_{60}$); we used this as the best approximation to the SIH of each individual. Finally, we also calculated the T_{max} difference from the beginning to the end of the TRP ($\Delta T_{TRP} = T_{300} - T_{60}$) in order to have a more detailed description of the animals' physiological response during a period of reduced stress-promoting stimulation.

Statistical analysis

We used R statistical environment (R Core Team, 2021) and SPSS software (v. 25.0. Armonk, NY: IBM Corp.) for all statistical analyses. Statistical significance was assumed at the 5% level. For parametric tests, data were evaluated for normality and homogeneity using the Kolmogorov-Smirnov test when sample size was greater than 30 and the Shapiro-Wilk test for smaller sample sizes, in combination with graphical methods (QQ-plots) and Levene's test. All the assumptions required for the post hoc tests were met, while data are expressed as means ± standard deviation (SD). Statistical significance was assumed at the 5% level.

Time series analysis

In order to examine the trend of eye temperature with time during our experimental protocol, we used time series analyses for groups of different trapping history. Initially, we plotted T_{max} using a loess smoothing function to visually assess the trend. Because our manipulations are sequential to each other and in the same order across all individuals, the T_{max} values for EMP and the T_{max} values for TRP are autocorrelated. Therefore, we used an adaptation of the Auto Regressive Integrated Moving Average (ARIMA) approach to modeling time series (Box et al., 2016), the SARIMA(p, d, q) (P, D, Q)S model. This model constructs a seasonal time-series model, with seasonality; in our case this refers to the pattern changes at intervals during the EMP and TRP. There are seven parameters to be considered when fitting the SARIMA model: p, the order of autoregression; d, the degree of difference; q, the moving average; P, the seasonal autoregression; D, the degree of seasonal difference; Q, the seasonal moving average and S, the seasonal period. Before fitting the SARIMA models, for the time series of each trapping history group, we identified significant lags using the autocorrelation and partial autocorrelation functions to assess stationarity, using both graphical and statistical methods. In cases in which stationarity was not met, we stabilized the T_{max} sequence by transforming the series using one-order differences to remove autocorrelation. Afterward, we re-assessed stationarity with the Augmented-Dickey Fuller (ADF) test (Gerolimetto and Magrini, 2017) and the Kwiatowski-Phillips-Schmidt (KPSS) test, while we visualized decomposition of seasonal, trend, and remainder components ("white noise") using the STL method (Cleveland et al., 1990). Then, we used an automated algorithm, the `auto.arima` (Hyndman and Khandakar, 2008) in R, to generate the optimal order of the p, d, q, P, D, and Q parameters by testing all potential models. We used the lowest Akaike Informa-

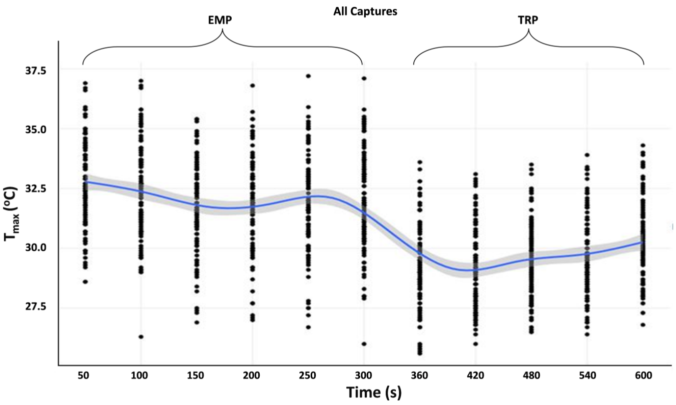

Figure 3 – Smoothed curve of T_{max} (°C) of all *A. mystacinus* captures during the two phases (EMP, TRP) of the experimental procedure. The time interval of 50 s between successive values during EMP corresponds to each experimental manipulation, while the 60 s interval during TRP represents T_{max} per 60 s in the box. Blue line: loess smoothed curve of mean T_{max} with 95% CI (gray).

tion Criterion (AIC) estimate to identify the model with the highest accuracy and we performed diagnostic checking, including residual analysis (Ljung-Box test). Additionally, we selected root-mean-square error (RMSE) and mean absolute error (MAE) to evaluate the models. For the time series analyses we used the following packages for data visualization and manipulation: `ggplot2` (Wickham, 2009), `tseries` (Trapletti and Hornik, 2019), `chron` (James and Hornik, 2020), `FitAR` (McLeod and Zhang, 2008), `forecast` (Hyndman et al., 2021), and `fpp2` (Hyndman, 2018).

Time series comparison

After model selection, we compared the derived stationary time series for groups with different trapping history in order to identify similarities between them. Time series data similarity patterns can be understood from mathematical functions named similarity measures (Cleasby et al., 2019). However, similarity measures can be used to compare the similarity between different pairs of time series (Cleasby et al., 2019) and for this reason we could not compare time series for sex or breeding condition for which we had only one pair of curves.

A widely used similarity measure involves the Dynamic Time Warping (DTW) algorithm (Senin, 2008) which we implemented using the `dtw` library in R (Giorgino, 2009). DTW is a fundamental technique in time series analysis for comparing a pair of curves using an elastic time-warping function which finds the optimal alignment between two temporal sequences. DTW calculates the distance between each possible pair of points allowing one-to-many mapping, leading to estimation of the optimal warping path (Senin, 2008; Müller, 2007). Shorth DTW distances signify a high similarity between two time series. For the computation and visualization of DTW alignments, we initially estimated the differenced value of each T_{max} of two temporal stationary sequences by calculating the amplitude at time T_{BW} (50 s) of the first time series with the amplitude of the second time series at time $T_{BW}+1(T_{CL})$, and $T_{BW}-1$ or $T_{BW}+2(T_{HFL})$ and $T_{BW}-2$, termed "local cost", and then we plotted the optimal warping path, the one with the minimum sum of all the local costs. Finally, we plotted the optimal alignments of the stationary models in the three-way form and we extracted the distance and the normalised distance values for each pair of examined time series.

Testing for differences in T_{max} and for the effect of body size on ΔT_{SIH}

Differences in mean and range of T_{max} during the two manipulation phases were examined using t-tests. Welch one-way analysis of variance was used to determine whether ΔT_{SIH} significantly differentiated according to trapping history. For post hoc examination of statistical differences we used Games-Howell tests. The effect of the time interval between first capture and recaptures on ΔT_{SIH} was tested using linear regression. The dependence of ΔT_{SIH} from morphometric traits was investigated using multilinear regression analysis, with a backward elimination procedure for significant variable selection, ensuring there was no violation of any of the required assumptions. For this analysis we used the first captures dataset, both as a whole and by each sex separately, because first captures had had no previous contact with humans or the manipulation procedure, whereas recaptures might be affected by animals' prior experience. We further tested the effect of body size on each of the two components of ΔT_{SIH}, T_{BW} and T_{60}, independently.

Table 1 – Mean and range of T_{max} values of each *A. mystacinus* individual, for groups according to sex, recapture status, and breeding condition, in the two phases of the manipulation procedure (EMP and TRP). Also shown is the 95% confidence interval (95% CI) for the difference between EMP and TRP and the result of paired samples t-tests (t) for the two phases.

(a) Mean T_{max} of each individual		$T_{meanEMP}$		$T_{meanTRP}$				
	n	Mean	SD	Mean	SD	95% CI	t	df
Males	50	32.02	2.21	29.50	1.79	2.14, 2.88	13.63**	49
Females	53	32.19	1.49	29.72	1.45	2.14, 2.79	15.19**	52
First Captures	27	32.19	1.94	29.47	1.39	2.27, 3.17	12.46**	26
1st Recaptures	22	31.22	1.80	29.41	1.66	1.32, 2.29	7.74**	21
2nd Recaptures	19	32.47	1.84	30.21	1.76	1.63, 2.90	7.52**	18
3rd Recaptures	14	32.49	2.12	29.53	2.02	2.24, 3.66	8.98**	13
Breeding	53	31.48	1.76	29.21	1.58	1.95, 2.58	14.24**	52
Non-breeding	50	32.73	1.81	30.03	1.55	2.33, 3.06	14.83**	49
All Captures	103	32.11	1.87	29.62	1.62	0.28, 0.73	4.49**	102

(b) Range of T_{max} of each individual		$T_{meanEMP}$		$T_{meanTRP}$				
	n	Mean	SD	Mean	SD	95% CI	t	df
Males	50	2.31	0.86	1.62	0.66	0.40, 0.98	4.78*	49
Females	53	1.95	0.82	1.61	0.80	0.00, 0.67	1.96	52
First Captures	27	2.18	1.07	1.65	0.65	0.04, 1.01	2.23*	26
1st Recaptures	22	2.00	0.59	1.58	0.70	−0.02, 0.85	1.97	21
2nd Recaptures	19	2.20	0.97	1.38	0.55	0.25, 1.37	3.07*	18
3rd Recaptures	14	2.13	0.76	1.94	1.19	−0.68, 1.07	0.47	13
Breeding	53	2.16	0.83	1.64	0.65	0.23, 0.81	3.66**	52
Non-breeding	50	2.08	0.88	1.59	0.81	0.13, 0.84	2.74*	49
All Captures	103	2.12	0.85	1.61	0.73	0.28, 0.73	4.49**	102

* $p<0.05$
** $p<0.001$

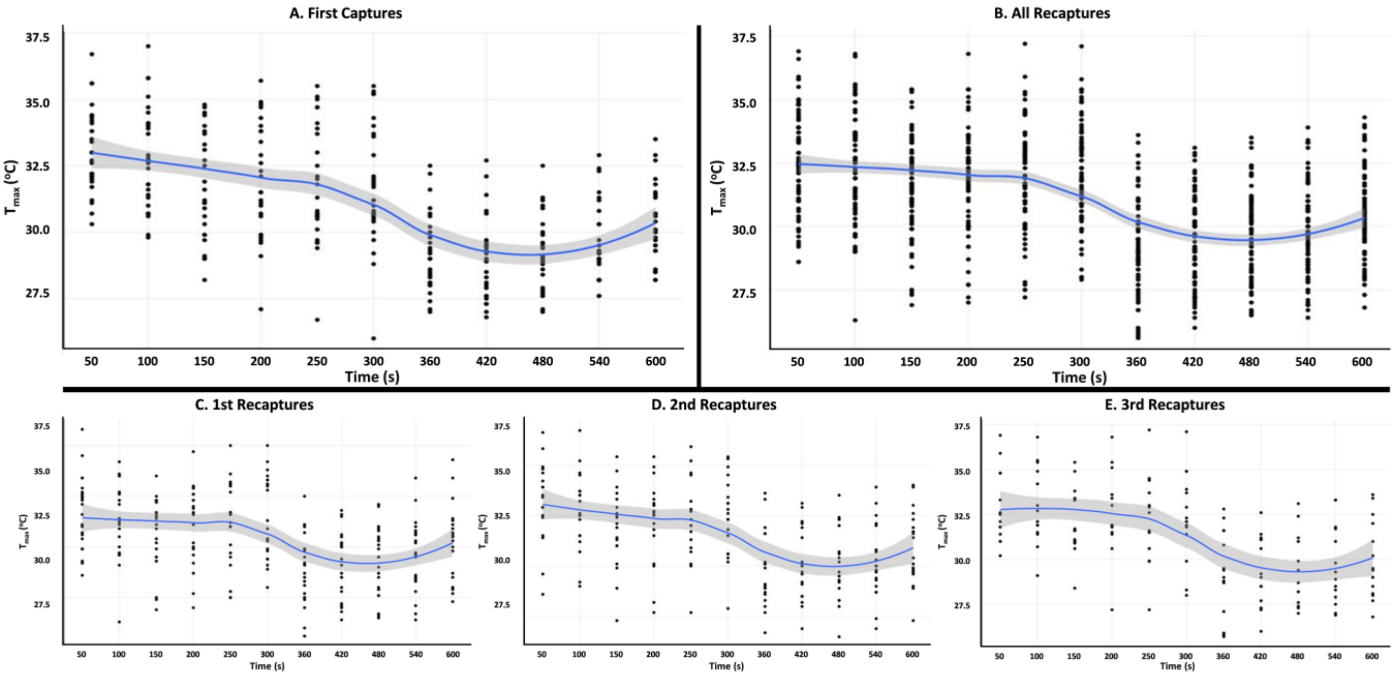

Figure 4 – Smoothed curves of T_{max} (°C) of the different trapping history subsets during the two phases (EMP, TRP) of the experimental procedure. The time interval of 50 s between successive values during EMP corresponds to each experimental manipulation, while the 60 s interval during TRP represents the eye temperature per 60 s in the box. Blue line: loess smoothed curve of mean T_{max} with 95% CI (gray).

Results

Individual differences in T_{max} mean and range between EMP and TRP

A total of 618 IR images were obtained and analysed for the EMP and 515 for the TRP, relating to 103 animals (76 of them were recaptures), 50 males and 53 females, 53 in breeding condition and 50 in non-breeding condition. $T_{meanEMP}$ of all 103 captures varied between 27.6 and 36.6 (32.11±1.87) °C, $T_{meanTRP}$ between 26.7 and 33.4 (29.62±1.62) °C, $T_{rangeEMP}$ varied between 0.5 and 5.2 (2.12±0.85) °C, and $T_{rangeTRP}$ between 0.4 and 5.2 (1.61±0.73) °C. $T_{meanEMP}$ differed significantly from $T_{meanTRP}$ of the same individual whether for the full data set or when checked with respect to sex, trapping history or breeding condition (Tab. 1a). Similarly, statistically significant differences existed between the $T_{rangeEMP}$ and $T_{rangeTRP}$, except for females, and 1st and 3rd recaptures (Tab. 1b). Detailed descriptive statistics of T_{max} with respect to sex, trapping history and breeding condition during the EMP and the TRP, are presented in Tab. S1 in the Supplemental Material.

Determination of time-series models of T_{max}

The curves in Fig. 3 and 4 show the temporal evolution of T_{max} during the EMP and TRP for different subsets of the data. In all cases T_{max} demonstrated an overall decreasing trend over time; however, there is a discernible upward trend in the latter part of TRP, especially after 420 s. Plots of the decomposed time series with the eliminated trend

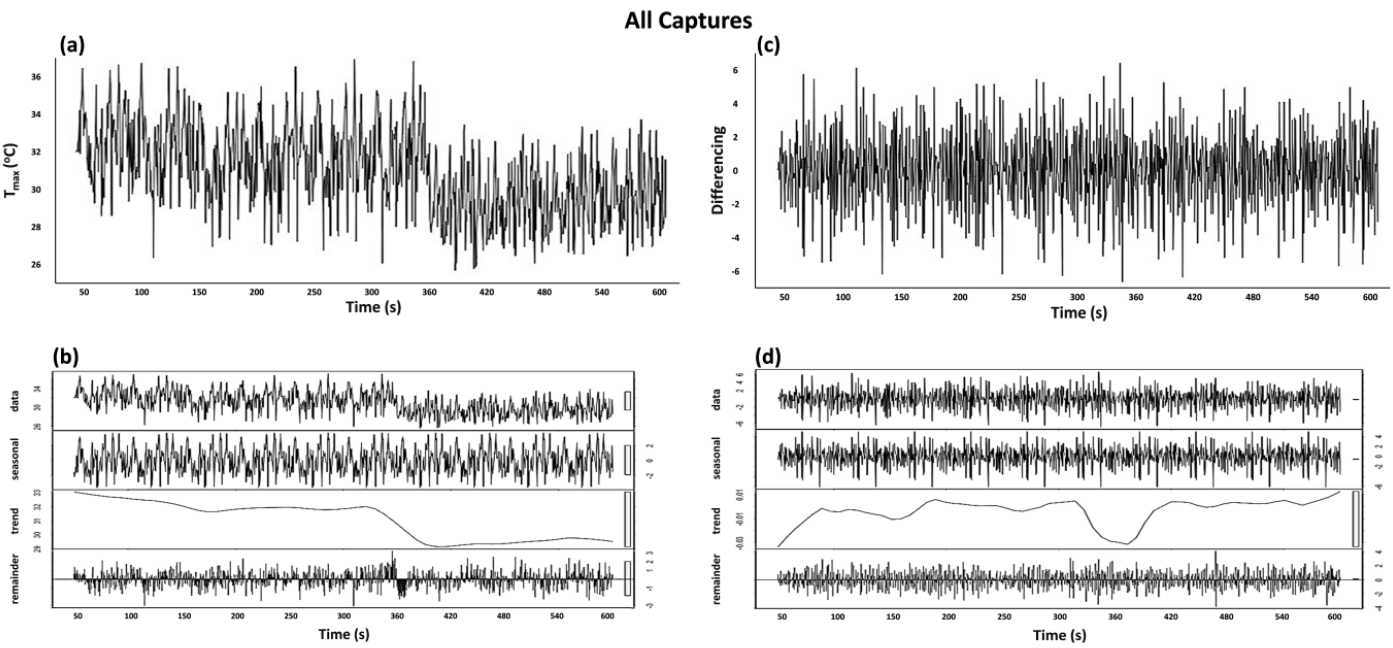

Figure 5 – Time series components for the whole dataset: (a) the non-stationary model; (b) variation of each component ("trend", "seasonal", "remainder") of the non-stationary model; (c) the stationary model obtained by taking one order difference to induce stationarity; (d) variation of each component of the stationary model. Y-axis represents T_max (°C) while X-axis represents time during the combined two phases of our experimental protocol.

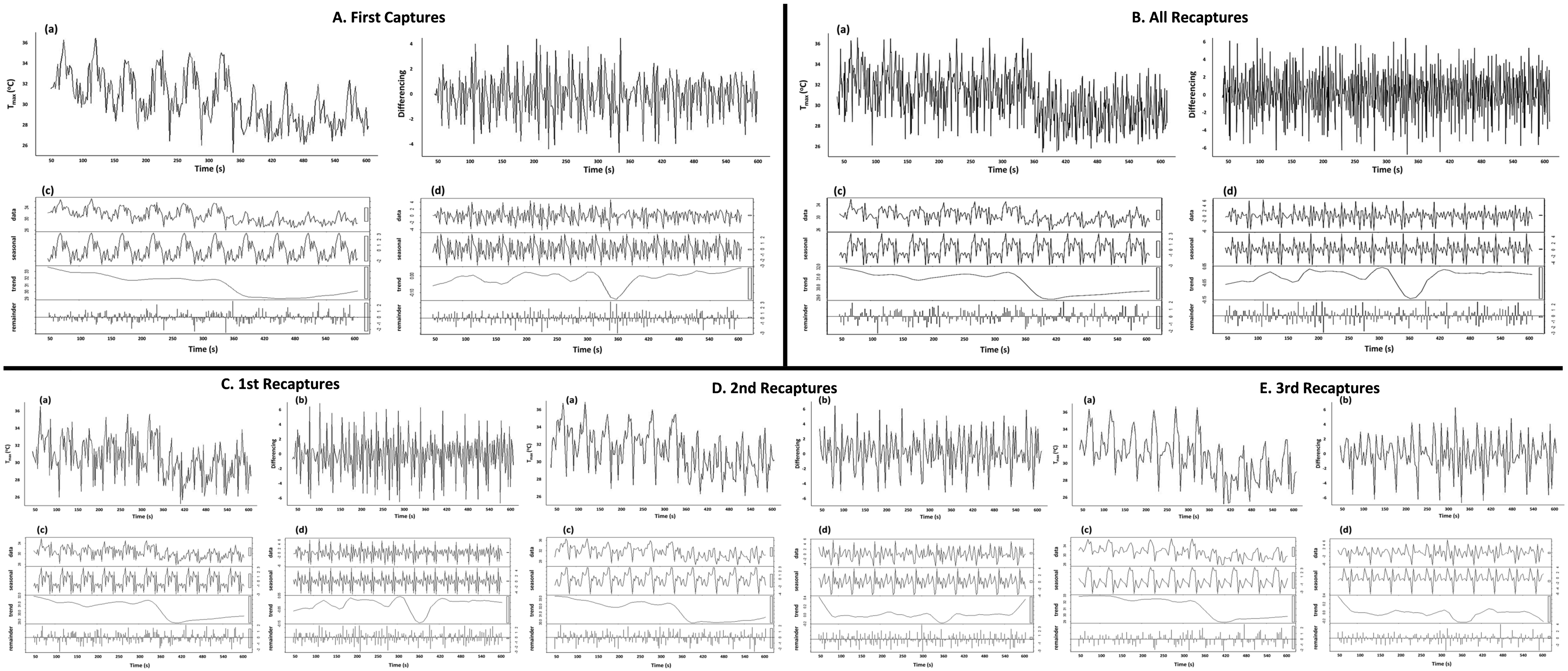

Figure 6 – Time series components for each trapping history subset: (a) the non-stationary model; (b) variation of each component ("trend", "seasonal", "remainder") of the non-stationary model; (c) the stationary model obtained by taking one order difference to induce stationarity; (d) variation of each component of the stationary model. Y-axis represents T_{max} (°C) while X-axis represents time during the combined two phases of our experimental protocol.

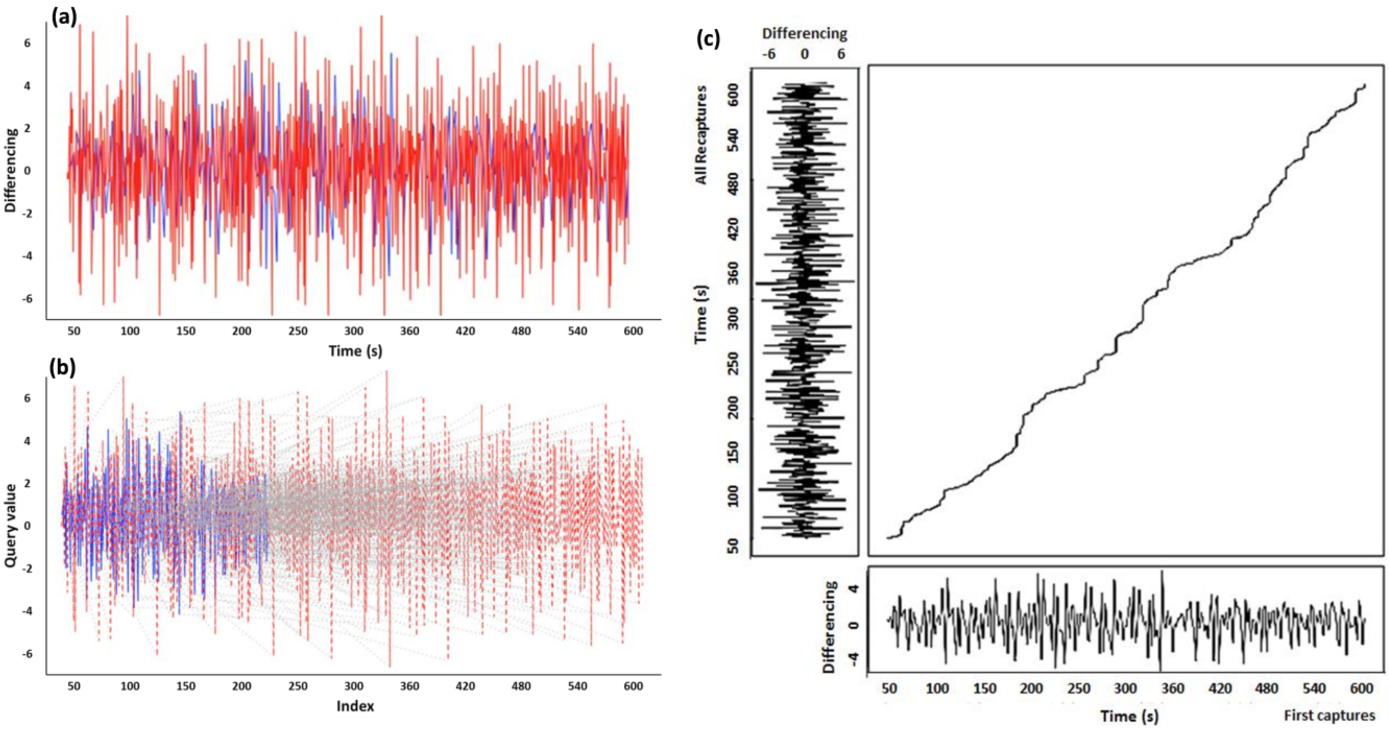

Figure 7 – Mapping of the stationary sequences for First Captures (blue) and All Recaptures (red); (a) the two time series plotted together, (b) the step pattern object which lists the allowed transitions in parallel with minimum-distance search, which characterizes the matching model, and (c) the minimum-distance warp path plotted in a three way form.

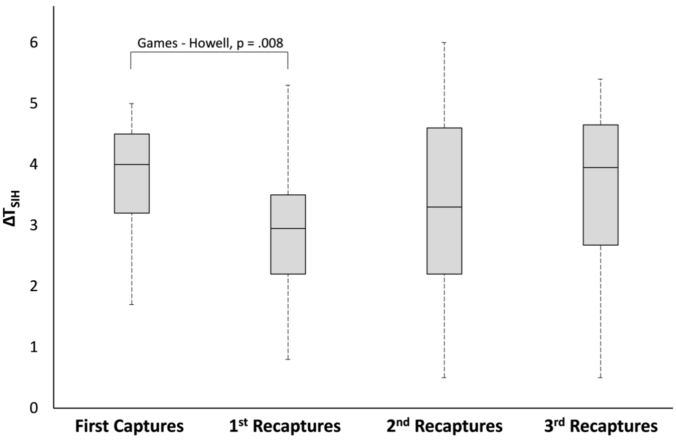

Figure 8 – Box plots and the Games-Howell post hoc test showing the ΔT_{SIH} differences between the four capture occasions. Horizontal lines represent the medians, boxes represent the interquartile ranges (25–75%) and whiskers represent data ranges.

are shown in Fig. 5 and 6. As can be seen in Fig. 5b and Fig. 6Ab – 6Eb, the trend component shows a very distinct 'step' after the end of the EMP, approximately from 300 s to 420 s, corresponding to the release of the animals in the RB. For the full dataset (all captures) the model with the lowest AIC, selected by the algorithm, was (0,0,1)(0,1,0)[103] (AIC=2499.11). The order of autoregression (p) was 0, the moving average (q) was 1, the degree of difference (d) was 0, the seasonal autoregression (P) was 0, the seasonal moving average (Q) was 0, and the degree of seasonal difference (S) was 1.

In all models, the converted time series showed stability improvement after differencing, as can be seen from the results of the stationarity tests (Tab. 2). In particular, the ADF and the KPSS tests showed consistency with the time-series plots, with a symmetrical oscillation of the series around the overall trend. The models for trapping history subsets, as well as the Goodness of Fit statistics, are shown in Tab. 3. For all the auto-fitted models, i.e., for First captures, All Recaptures, and for 1st, 2nd and 3rd Recaptures, the Ljung-Box test p-value was >0.05 (Tab. 3), indicating a good fit. The MSE and the RMSE displayed low values (Tab. 3), also indicating a high degree of fit of the derived stationary time series. The stationary models have attained a relatively flat trend component, as intended by the differencing procedure, but a noticeable "dent" remained after the end of the EMP, attributable to the sudden drop in T_{max} between 300 s and 420 s (Fig. 5d and Fig. 6Ad – 6Ed).

Additional test results and plots related to the conversion of non-stationary to stationary models are shown in Tab. S2 and Fig. S1 and S2 in the Supplemental Material.

Comparison of time series for different trapping history

For each time series pair, the DTW algorithm recursively searched all eye temperatures combinations to identify the path of minimum distance. The plotted optimal warping paths of the T_{max} values of EMP and TRP started with T_{BW} of the first examined first capture individual

Table 2 – Stationarity tests before and after differencing the time series.

	KPSS trend		KPSS level		ADF	
Stationarity tests	**Initial**	**Differenced**	**Initial**	**Differenced**	**Initial**	**Differenced**
All Captures	0.01	0.01	0.01	0.1	0.01	0.1
First captures	0.01	0.05	0.1	0.1	0.01	0.1
All Recaptures	0.01	0.01	0.01	0.1	0.01	0.1
1st Recaptures	0.01	0.01	0.01	0.1	0.01	0.1
2nd Recaptures	0.01	0.01	0.01	0.1	0.01	0.1
3rd Recaptures	0.01	0.01	0.01	0.1	0.01	0.1

Table 3 – SARIMA models for the full dataset and its different subsets. Models with a Ljung-Box Q test p-value >0.05 are a good fit for the dataset.

		Goodness-of-Fit Statistics			Ljung-Box Q Test	
***A. mystacinus* Groups**	**Models**	**AIC**	**RMSE**	**MAE**	**Statistic**	**p-value**
All Captures	(0,0,1)(0,1,0)[103]	2499.11	0.88	0.61	408.32	<0.05
First Captures	(0,0,1)(2,1,0)[27]	623.03	0.80	0.58	104.17	>0.05
All Recaptures	(0,0,1)(1,1,0)[76]	1840.82	0.87	0.62	172.71	>0.05
1^{st} Recapture	(0,0,1)(2,1,0)[22]	531.97	0.85	0.62	60.504	>0.05
2^{nd} Recapture	(0,0,1)(0,1,1)[19]	483.74	0.91	0.66	64.034	>0.05
3^{rd} Recapture	(1,0,1)(0,1,1)[14]	398.94	1.06	0.79	22.935	>0.05

and with the first examined first recaptured individual, and reached to T_{300} of the T_{RP} for each individual. DTW aligned these trajectories by creating a distance matrix in which the smallest distance between these T_{max} represented the cost of aligning them. The total cumulative distance between them (optimal warping path), which must be contiguous and monotonic, ended at the sequence tails (top-right corner of the matrix) and provided their alignment (Fig. 7, S3 – S5). Computation of the minimum distance and normalised distances showed that the "First Captures — All Recaptures" had the lowest similarity of all the examined pairs of time series (Distance value=1247.7; Normalised Distance value=1.21), which is caused by the inclusion of all recapture events, even beyond the 3rd recapture (n=76). A greater similarity was observed in the time series pair "First captures — 2nd Recaptures" (Distance value=395.9; Normalised Distance value=0.86) compared with the pair "First Captures — 3rd Recaptures" (Distance value=407.6; Normalised Distance value=0.99) or the pair "First Captures — 1st Recaptures" (Distance value=477.1; Normalised Distance value=0.97).

Eye temperature differences at key points of the experimental procedure

The temperature difference between the beginning of EMP and the beginning TRP (ΔT_{SIH}), for all captures, ranged from 0.5 to 6.6 (3.50±1.29) °C. Comparing groups of different trapping history, Welch one-way ANOVA gave statistically significant differences in ΔT_{SIH} ($F_{3, 35}$=5.39; p=0.004). Games-Howell post-hoc analysis showed that first captures differed significantly from 1st recaptures but there was no significant difference between first captures and 2nd or 3rd recaptures (Fig. 8). ΔT_{SIH} was found to depend on the time interval between the first capture and the 2nd and 3rd recaptures ($F_{1, 27}$=12.75; p<0.001; R^2_{adj}=0.296). In terms of eye temperature differences during TRP (i.e., between T_{60} and T_{300}), ΔT_{TRP} varied between -2.2 to 4.4 (1.01±1.18) °C; no differences were observed between sexes (t_{101}=-0.736; p>0.05), reproductive condition (t_{101}=-0.627; p>0.05), or capture events ($F_{3, 78}$=0.409; p>0.05).

Effect of body size on ΔT_{SIH}

´ Single morphometric traits or combinations of traits are statistically significant predictors of ΔT_{SIH}. Specifically, for the total of first captures the model was statistically significant ($F_{2, 24}$=30.27; p<0.001). ΔT_{SIH} increases with decreasing body size (Tab. 4). In the two sex subsets, there were statistically significant models for both first capture males ($F_{1, 14}$=30.94; p<0.001; R^2=0.667), and first capture females ($F_{1, 9}$=16.56; p=0.003; R^2=0.609). HBL was the only statistically significant explanatory variable, with ΔT_{SIH} also decreasing with body size (Tab. 4).

Repeating the above analysis for T_{BW} and T_{60} independently, statistically significant results were obtained only for T_{BW} for all first captures and for first capture males, but not females. BW was the only statistically significant explanatory variable for all first captures [$T_{BW} = 36.72 + (-0.096BW)$; $F_{1, 25}$=5.75; p=0.024; R^2_{adj}=0.155] and HBL for first capture males [$T_{BW} = 47.08 + (-1.47HBL)$; $F_{1, 14}$=5.97; p=0.027; R^2_{adj}=0.237]. In both cases, R^2_{adj} values were much lower than with ΔT_{SIH}.

Discussion

In this study we investigate the influence of a standard field procedure on the maximum eye temperature of a wild rodent, as an index of stress, in field conditions. Handling and trapping have been shown to cause stress in rodents, both in the laboratory (Long et al., 1990; Briese and De Quijada, 1970) and in the wild (Fletcher and Boonstra, 2006). The physiological response is related to duration of capture (Bosson et al., 2012) but it can be caused by even short-term handling (Gelling et al., 2009). The observed rise in body temperature as a physiological response to handling is a regulated process to be taken into consideration in research involving the manipulation of rodents (Groenink et al., 1994; Nakamori et al., 1993; Long et al., 1990). We provide substantial evidence, obtained non-invasively, for a pattern of A. mystacinus physiological response to manipulations.

Eye temperature differences observed between the EMP and the TRP appeared in all subsets of individuals examined, as did the decrease of eye temperature after completion of the experimental manipulations (Fig. 3, 4). These responses appear to be a very robust but at the same

Table 4 – Final models obtained from multiple linear regression analyses using a backward procedure on morphometric traits as explanatory variables of ΔT_{SIH} variation. All models were statistically significant (p<0.05).

Group	Response variable	Predictor variable	B	SE B	β	t	p	Adj. R^2	F
First Captures	ΔT_{SIH}	(constant)	14.93	1.80		8.28	0.00	0.692	30.27
		CL	−1.09	0.41	−0.28	−2.64	0.01		
		HBL	−0.74	0.10	−0.78	−7.19	0.00		
	Predictive regression equation	$\Delta T_{SIH} = 14.93 + (-1.09CL) + (-0.74HBL)$							
First Captures – Males	ΔT_{SIH}	(constant)	13.92	1.84		7.57	0.00	0.666	30.94
		HBL	−1.06	0.19	−0.83	−5.56	0.00		
	Predictive regression equation	$\Delta T_{SIH} = 13.92 + (-1.06HBL)$							
First Captures – Females	ΔT_{SIH}	(constant)	9.41	1.31		7.14	0.00	0.609	16.56
		HBL	−0.60	0.14	−0.80	−4.07	0.00		
Predictive regression equation		$\Delta T_{SIH} = 9.41 + (-0.60HBL)$							

time complex phenomenon. During the TRP there was a gradual increase in T_{max}, peaking at the end of this phase though there was no statistically significant differentiation of ΔT_{TRP} as to sex, trapping history or breeding condition, suggesting a rather uniform response of all animals to their stay in the RB. We suggest that the difference observed between the EMP and the TRP may be related to the different quality of stressing stimuli as perceived by the animals. Handling during the EMP is more likely to be perceived as an encounter with a predator (Hernández et al., 2018; Beale and Monaghan, 2004; Frid and Dill, 2002) while the stay in the RB was more likely to induce a frustration-like state (Mason, 2006; Amsel, 1958), displaying stereotypical behavioural patterns such as freezing, grooming and attempts to find an escape route, coinciding with a mildly but clearly rising eye temperature (Fig. 3, 4).

An important finding of the time series analysis is the common pattern of the trend component in all subsets of the data, with a sudden decrease of T_{max} after the end of manipulations. This pattern was retained even after conversion to the stationary time series models. This is a clear manifestation of the relaxation experienced when animals were placed in the RB, however, in all cases examined, the sudden drop in T_{max} was followed by a slight upward trend. A similar effect of waiting has been known to cause a rapid increase (i.e., within seconds) in body temperature as part of the stress response of laboratory mice (Clement et al., 1989). Thus, a longer stay in the RB would not be likely to induce a further drop in stress levels. Consequently, a short stay of up to about two minutes, sufficient for taking the necessary IR images, would be recommended for implementation of our method.

The high variability among individuals' eye temperature for each experimental manipulation during EMP can be affected by either or both of two factors: the way animals are manipulated during the different measurements, and the time elapsed during the manipulation procedure. Regarding the first factor, initially, each individual was firmly grasped behind the nape with the index and thumb fingers, as recommended by small mammal handling protocols (Sikes and Gannon, 2011), and then the animal was placed in a different posture, depending on the manipulation, without touching a solid surface. BW, CL, HFL, and EL were measured with the animal's body inclined, while HBL and TL with the animal upside down. The lowest T_{max} occurred when measuring HBL, while the highest T_{max} occurred on measuring BW on the first 50 s of handling (Fig. 3 and Tab. S1 in Supplemental Material). Since these manipulations were in the same fixed order for all subjects, we cannot check the effect of each one on its own. In terms of the second factor, we tested the effect of time elapsed on the range of values among individuals at each time interval using a simple linear regression model. The result was a strong positive effect during the EMP for first captures ($F_{1,4}$=24.70; p=0.008; R^2=0.823) but not statistically significant for EMP of recaptures nor for TRP of either first captures or recaptures, nor was there any apparent connection when tested with respect to sex or breeding condition. A possible explanation for this could be a more variable response to handling in first captures compared with recaptures but there are many confounding factors that may also be responsible for these variations. Since a variety of stressors such as the length of time spent in live traps (Harper and Austad, 2000), predator presence (Navarro-Castilla and Barja, 2014), reproduction (Barja et al., 2011), social environment and dominance (Avitsur et al., 2003; Creel, 2001), habitat change due to grazing (Navarro-Castilla et al., 2017), food availability (Navarro-Castilla and Barja, 2019), age at first exposure to a stressor (Beery and Kaufer, 2015), and the way animals perceive stressors (Lucas et al., 2014) have been shown to affect animals in the wild, we believe that further research is required towards a better understanding of this result.

To assess SIH it is necessary to have temperature measurements both when the animal is calm and when it is stressed. Established protocols for measuring SIH (Van Der Heyden et al., 1997; Borsini et al., 1989) are not applicable in field conditions. For this reason we tried to follow the protocol described by Careau et al. (2012), at least in terms of the time frame of the IRT readings simultaneously with the manipulations, but our protocol (a) enhances the importance of the first moment of handling a wild animal, (b) emphasises the significance of obtaining temperature values non-invasively using IRT, (c) provides time for the study animal to calm down, (d) uses eye temperature instead of rectal temperature, and (e) the measuring intervals are related to the duration of each manipulation (50 s per manipulation). We based the measurement of SIH (ΔT_{SIH}) on T_{max} at two critical points of the experimental procedure. These two points were the first moment when a wild rodent came into contact with a human being, on measuring TBW, and the first minute of the TRP (T_{60}) which immediately followed the most influential step of the experimental procedure — the release of the researcher's grasp and the return of the animal to solid footing. It should be noted that later during the TRP there was no further significant reduction in Tmax. A stay for more than 60 to 120 s in temporary confinement does not appear to be effective in further reducing the stress level of the animals.

The choice of measuring SIH in the way described is ideal for field conditions as it is relatively fast and simple to perform and has minimal impact on the animal's stress condition. Yet, SIH is a complex process (Nakamura, 2015; Olivier, 2015; McGivern et al., 2009; Peloso et al., 2002) and there is no standardised method for its assessment in field conditions. This lack of standardisation becomes apparent when examining the differences observed in ΔT_{SIH} in first captures in relation to recaptures. We were expecting that in all recaptures (1st, 2nd, 3rd) SIH would be lower than for the first capture due to increased familiarity of the animals with the procedure. In fact, we observed frequent recapture events, contra-indicating trap avoidance. However, the post hoc Games-Howell test for differences in ΔT_{SIH} showed that the first captures (ΔT_{SIH}=3.86 ± 0.80 °C) were significantly differentiated only from the 1st recaptures (ΔT_{SIH}=2.76 ± 1.03 °C) (Fig. 8). Paradoxically, in later recaptures, the SIH was almost the same as in first captures (ΔT_{SIH}=3.41 ± 1.50 °C for the 2nd and ΔT_{SIH}=3.65 ± 1.38 °C for the 3rd recapture). These results are confirmed by the comparisons of time series for animals with different trapping history, whereby a much higher dissimilarity measure was found in the "First captures — 1st recaptures" pair than in pairs comprising 2nd or 3rd recaptures (Fig. S3 – S5). Even though these findings contradict the results of Careau et al. (2012) on chipmunks (at least for 2nd and later recaptures), they may be explained by the effect of time elapsed between successive recaptures. This lends support to the hypothesis of several researchers (Yang et al., 2019; Gros and Wang, 2018; Cès et al., 2018), that rodents exhibit spatial and functional memory impairments which can start before old age sets in. Thus, mature *A. mystacinus* might experience long-term memory decline leading to 2nd and 3rd recapture SIH levels as high as on their first capture.

We consider that the dependence of ΔT_{SIH} from body size measures in first captures may provide valuable clues in the study of acute stress caused by handling. The manipulation procedure is a novel stressor that affects an animal's physiological response and which may be altered over subsequent recapture occasions (Boonstra, 2013; Fletcher and Boonstra, 2006) — this is the reason that recaptures were not used in the body size analysis. The high explanatory power of the linear regression models of ΔT_{SIH} on CL and HBL for first captures (both sexes R^2_{adj}=0.692; males R^2_{adj}=0.666; females R^2_{adj}=0.609) (Tab. 4) indicates a strong inverse dependence of the levels of stress on body size. The weak dependence of T_{BW} on body size measures, with lower explanatory power than for the ΔT_{SIH} models, and the absence of a statistically significant result for T_{60}, are in contrast with the above results. Therefore, the dependence of ΔT_{SIH} from body size appears not to be a simple consequence of different T_{max} at the beginning of the EMP or of the TRP for different body sizes but a combination of the two. The ability of mammals to control surface temperature increases with their body size due to their smaller surface-to-volume ratio (Gordon, 2017). Vasomotor control of the body surface temperature has been shown to be the most important way to achieve thermal homeostasis in mammals across a range of sizes from 20 g to 4000 kg (Phillips and Heath, 1995) but these effects are unlikely to be important in our case because body size variability of captured *A. mystacinus* was low (BW: $\bar{x}$=37.65, SD=7.16, interquartile range (IQR)=11.0; CL: $\bar{x}$=3.79, SD=0.21, IQR=0.30; HBL: $\bar{x}$=9.27, SD=0.84, IQR=1.1). A more likely explanation would be based on social dominance relationships, as has been shown for laboratory mice (Drews, 1993), presuming larger individuals tend to be nearer to the top of the hierarchy and, thus, be less stressed than smaller-sized ones. Future studies should focus on estimating a precise indicator, equivalent to the one described as "vasomotor index" (Phillips and Heath, 1995), for *A. mystacinus* (or any other rodent species) that includes the species' effective body surface area, its standard metabolic rate, core body temperature a critical body temperature. Our hypothesis may be strengthened, and interesting research questions may be raised concerning factors inducing stress in rodents with further field data. Eventually, this could also allow the development of improved trapping and handling protocols for wild rodents to minimise stress and its long-term side-effects, such as on survival or reproduction, in carrying out field studies.

To summarize, this study has shown that eye temperature, measured non-invasively, is an effective index for monitoring the physiological response of a wild rodent to manipulations in field conditions. A limitation of this method is the need for a short stay in calming conditions, such as our RB, to obtain an eye temperature measurement representing a relative calm state. The highest stress occurred at the start of the experimental manipulations i.e., in the beginning of the handling procedure. The lowest stress was found upon releasing the grip on the animal's nape and placing the animal on solid ground. Further keeping the animal in a confined unfamiliar space appeared to gradually increase stress. Trapping history and body size appear to affect the animals' physiology significantly and, thus, should be taken into account when using this method for monitoring SIH. The advantage of our experimental protocol was that the manipulated individuals were stressed solely by the human intervention and not by the methodological tools. IRT, when used on a wild rodent in field conditions, appears to give similar results to those found in studying stress in laboratory and captive animals and, thus, can be a very useful tool in Conservation Physiology studies and should be considered as a priority method for monitoring SIH non-invasively.

References

Amico J.A., Mantella R.C., Vollmer R.R., Li X., 2004. Anxiety and stress responses in female oxytocin deficient mice. J. Neuroendocrinol. 16(4): 319–324. doi:10.1111/j.0953-8194.2004.01161.x

Amsel A., 1958. The role of frustrative nonreward in noncontinuous reward situations. Psychol. Bull. 55(2): 102–119. doi:10.1037/h0043125

Avitsur R., Stark J.L., Dhabhar F.S., Kramer K.A., Sheridan J.F., 2003. Social experience alters the response to social stress in mice. Brain. Behav. Immun. 17(6): 426–437. doi:10.1016/S0889-1591(03)00034-5

Barja I., Silván G., Martínez-Fernández L., Illera J.C., 2011. Physiological Stress Responses, Fecal Marking Behavior, and Reproduction in Wild European Pine Martens (*Martes martes*). J. Chem. Ecol. 37(3): 253–259. doi:10.1007/s10886-011-9928-1

Bartolome E., Azcona F., Maria C.A., Perdomo-González D., Ribes-Pons J., Terán E., 2019. Testing eye temperature assessed with infrared thermography to evaluate stress in meat goats raised in a semi-intensive farming system: A pilot study. Arch. Anim. Breed. 62(1): 199–204. doi:10.5194/aab-62-199-2019

Beale C.M., Monaghan P., 2004. Human disturbance: People as predation-free predators? J. Appl. Ecol. 41(2): 335–343. doi:10.1111/j.0021-8901.2004.00900.x

Beery A.K., Kaufer D., 2015. Stress, social behavior, and resilience: Insights from rodents. Neurobiology of Stress, Elsevier.

Bittencourt M. de A., Melleu F.F., Marino-Neto J., 2015. Stress-induced core temperature changes in pigeons (*Columba livia*). Physiol. Behav. 139: 449–458. doi:10.1016/j.physbeh.2014.11.067

Blessing W.W., 2003. Lower brainstem pathways regulating sympathetically mediated changes in cutaneous blood flow. Cell. Mol. Neurobiol. 23(4–5): 527–538. doi:10.1023/A:1025020029037

Boonstra R., 2013. Reality as the leading cause of stress: Rethinking the impact of chronic stress in nature. Funct. Ecol. 27(1): 11–23. doi:10.1111/1365-2435.12008

Borsini F., Lecci A., Volterra G., Meli A., 1989. A model to measure anticipatory anxiety in mice? Psychopharmacology (Berl). 98(2): 207–211. doi:10.1007/BF00444693

Bosson C.O., Islam Z., Boonstra R., 2012. The impact of live trapping and trap model on the stress profiles of North American red squirrels. J. Zool. 288(3): 159–169. doi:10.1111/j.1469-7998.2012.00941.x

Bouwknecht J.A., Olivier B., Paylor R.E., 2007. The stress-induced hyperthermia paradigm as a physiological animal model for anxiety: A review of pharmacological and genetic studies in the mouse. Neuroscience and Biobehavioral Reviews. Pergamon.

Box G.E., Jenkins G.M., Reinsel G.C., Ljung G.M., 2016. Time series analysis: forecasting and control. John Wiley & Sons, Ltd., Chichester, West Sussex, UK.

Briese E., Cabanac M., 1991. Stress hyperthermia: Physiological arguments that it is a fever. Physiol. Behav. 49(6): 1153–1157. doi:10.1016/0031-9384(91)90343-M

Briese E., De Quijada M.G., 1970. Colonic temperature of rats during handling. Acta Physiol. Pharmacol. Latinoam. 20(2): 97–102.

Briscoe N.J., Handasyde K.A., Griffiths S.R., Porter W.P., Krockenberger A., Kearney M.R., 2014. Tree-hugging koalas demonstrate a novel thermoregulatory mechanism for arboreal mammals. Biol. Lett. 10(6): 20140235. doi:10.1098/rsbl.2014.0235

Burn C.C., Mason G.J., 2008. Effects of cage-cleaning frequency on laboratory rat reproduction, cannibalism, and welfare. Appl. Anim. Behav. Sci. 114(1–2): 235–247. doi:10.1016/j.applanim.2008.02.005

Buwalda B., Scholte J., de Boer S.F., Coppens C.M., Koolhaas J.M., 2012. The acute glucocorticoid stress response does not differentiate between rewarding and aversive social stimuli in rats. Horm. Behav. 61(2): 218–226. doi:10.1016/J.YHBEH.2011.12.012

Cabanac A., Briese E., 1992. Handling elevates the colonic temperature of mice. Physiol. Behav. 51(1): 95–98. doi:10.1016/0031-9384(92)90208-J

Careau V., Réale D., Garant D., Speakman J.R., Humphries M.M., 2012. Stress-induced rise in body temperature is repeatable in free-ranging Eastern chipmunks (*Tamias striatus*). J. Comp. Physiol. B Biochem. Syst. Environ. Physiol. 182(3): 403–414. doi:10.1007/s00360-011-0628-5

Cès A., Burg T., Herbeaux K., Héraud C., Bott J.B., Mensah-Nyagan A.G., Mathis C., 2018. Age-related vulnerability of pattern separation in C57BL/6J mice. Neurobiol. Aging 62: 120–129. doi:10.1016/j.neurobiolaging.2017.10.013

Church J.S., Hegadoren P.R., Paetkau M.J., Miller C.C., Regev-Shoshani G., Schaefer A.L., Schwartzkopf-Genswein K.S., 2014. Influence of environmental factors on infrared eye temperature measurements in cattle. Res. Vet. Sci. 96(1): 220–226. doi:10.1016/j.rvsc.2013.11.006

Cilulko J., Janiszewski P., Bogdaszewski M., Szczygielska E., 2013. Infrared thermal imaging in studies of wild animals. Eur. J. Wildl. Res. 59(1): 17–23. doi:10.1007/s10344-012-0688-1

Cleasby I.R., Wakefield E.D., Morrissey B.J., Bodey T.W., Votier S.C., Bearhop S., Hamer K.C., 2019. Using time-series similarity measures to compare animal movement trajectories in ecology. Behav. Ecol. Sociobiol. 73(11): 151. doi:10.1007/s00265-019-2761-1

Clement J.G., Mills P., Brockway B., 1989. Use of telemetry to record body temperature and activity in mice. J. Pharmacol. Methods 21(2): 129–140. doi:10.1016/0160-5402(89)90031-4

Cleveland R.B., Cleveland W.S., McRae J.E., Terpenning I., 1990. STL: A seasonal-trend decomposition. J. Off. Stat. 6(1): 3–73.

Cook N., Schaefer A., Warren L., Burwash L., Anderson M., Baron V., 2001. Adrenocortical and metabolic responses to ACTH injection in horses An assessment by salivary cortisol and infrared thermography of the eye. Can. J. Anim. Sci. 81(4): 621.

Cook N.J., Church J.S., Schaefer A.L., Webster J.R., Suttie J.M.M., 2005. Stress and pain assessment of velevet antler removal from Elk (*Cervus elaphus canadensis*) and Reindeer (*Rangifer tarandus*). Online J. Vet. Res. 9: 13–25.

Creel S., 2001. Social dominance and stress hormones. Trends Ecol. Evol. 16(9): 491–497. doi:10.1016/S0169-5347(01)02227-3

Crestani C.C., 2016. Emotional stress and cardiovascular complications in animal models: A review of the influence of stress type. Front. Physiol. 7(June). doi:10.3389/fphys.2016.00251

Dallmann R., Steinlechner S., Von Hörsten S., Karl T., 2006. Stress-induced hyperthermia in the rat: Comparison of classical and novel recording methods. Lab. Anim. 40(2): 186–193. doi:10.1258/002367706776319015

Dantzer B., Fletcher Q.E., Boonstra R., Sheriff M.J., 2014. Measures of physiological stress: A transparent or opaque window into the status, management and conservation of species? Conserv. Physiol. 2(1): 1–18. doi:10.1093/conphys/cou023

Dantzer B., Santicchia F., Van Kesteren F., Palme R., Martinoli A., Wauters L.A., 2016. Measurement of fecal glucocorticoid metabolite levels in Eurasian red squirrels (*Sciurus vulgaris*): Effects of captivity, sex, reproductive condition, and season. J. Mammal. 97(5): 1385–1398. doi:10.1093/jmammal/gyw095

Drews C., 1993. The concept and definition of dominance in animal behaviour. Behaviour 125(3–4): 283–313. doi:10.1163/156853993X00290

Dunbar M.R., Johnson S.R., Rhyan J.C., McCollum M., 2009. Use of infrared thermography to detect thermographic changes in mule deer (*Odocoileus hemionus*) experimentally infected with foot-and-mouth disease. J. Zoo Wildl. Med. 40(2): 296–301. doi:10.1638/2008-0087.1

Edgar J.L., Lowe J.C., Paul E.S., Nicol C.J., 2011. Avian maternal response to chick distress. Proc. R. Soc. B Biol. Sci. 278(1721): 3129–3134. doi:10.1098/rspb.2010.2701

Engel G.L., Schmale A.H., 1972. Conservation-withdrawal: a primary regulatory process for organismic homeostasis. Ciba Found. Symp. 8: 57–75. doi:10.1002/9780470719916.ch5

Faye E., Dangles O., Pincebourde S., 2016. Distance makes the difference in thermography for ecological studies. J. Therm. Biol. 56: 1–9. doi:10.1016/j.jtherbio.2015.11.011

Fletcher Q.E., Boonstra R., 2006. Impact of live trapping on the stress response of the meadow vole (*Microtus pennsylvanicus*). J. Zool. 270(3): 473–478. doi:10.1111/j.1469-7998.2006.00153.x

Frid A., Dill L., 2002. Human-caused disturbance stimuli as a form of predation risk. Ecol. Soc. 6(1): 11. doi:10.5751/es-00404-060111

Gelling M., McLaren G.W., Mathews F., Mian R., Macdonald D.W., 2009. Impact of trapping and handling on Leukocyte Coping Capacity in bank voles (*Clethrionomys glareolus*) and wood mice (*Apodemus sylvaticus*). Anim. Welf. 18(1): 1–7.

Gerolimetto M., Magrini S., 2017. On the power of the simulation-based ADF test in bounded time series. Econ. Bull. 37(1): 539–552.

Giorgino T., 2009. Computing and visualizing dynamic time warping alignments in R: The `dtw` package. J. Stat. Softw. 31(7): 1–24. doi:10.18637/jss.v031.i07

Gjendal K., Franco N.H., Ottesen J.L., Sørensen D.B., Olsson I.A.S., 2018. Eye, body or tail? Thermography as a measure of stress in mice. Physiol. Behav. 196: 135–143. doi:10.1016/j.physbeh.2018.08.022

Gordon C.J., 2017. The mouse thermoregulatory system: Its impact on translating biomedical data to humans. Physiology and Behavior, Elsevier Inc.

Groenink L., van der Gugten J., Zethof T., van der Heyden J., Olivier B., 1994. Stress-induced hyperthermia in mice: Hormonal correlates. Physiol. Behav. 56(4): 747–749. doi:10.1016/0031-9384(94)90237-2

Gros A., Wang S.H., 2018. Behavioral tagging and capture: long-term memory decline in middle-aged rats. Neurobiol. Aging 67: 31–41. doi:10.1016/j.neurobiolaging.2018.02.023

Harper J.M., Austad S.N., 2000. Fecal glucocorticoids: A noninvasive method of measuring adrenal activity in wild and captive rodents. Physiol. Biochem. Zool. 73(1): 12–22. doi:10.1086/316721

Harper J.M., Austad S.N., 2001. Effect of capture and season on fecal glucocorticoid levels in deer mice (*Peromyscus maniculatus*) and red-backed voles (*Clethrionomys gapperi*). Gen. Comp. Endocrinol. 123(3): 337–344. doi:10.1006/gcen.2001.7682

Herborn K.A., Jerem P., Nager R.G., McKeegan D.E.F., McCafferty D.J., 2018. Surface temperature elevated by chronic and intermittent stress. Physiol. Behav. 191: 47–55. doi:10.1016/j.physbeh.2018.04.004

Hernández M., Navarro-Castilla Á., Piñeiro A., Barja I., 2018. Wood mice aggressiveness and flight response to human handling: Effect of individual and environmental factors. Ethology 124(8): 559–569. doi:10.1111/eth.12760

Horton K.G., Shriver W.G., Buler J.J., 2015. A comparison of traffic estimates of nocturnal flying animals using radar, thermal imaging, and acoustic recording. Ecol. Appl. 25(2): 390–401. doi:10.1890/14-0279.1.sm

Hyndman R.B., Khandakar Y., 2008. Automatic Time Series Forecasting: The `forecast` Package for R. J. Stat. Softw. 27(3): 22.

Hyndman R.J., Athanasopoulos G., Bergmeir C., Caceres G., Chhay L., O'Hara-Wild M., Petropoulos F., Razbash S., Wang E., Yasmeen F., 2021. Package `forecast`: Forecasting functions for time series and linear models, Software, R package version 8.17.0. Available at: https://pkg.robjhyndman.com/forecast/

Hyndman R., 2018. Package `fpp2`: Data for "Forecasting: Principles and Practice". R package version 2.292. Available at: https://CRAN.R-project.org/package=fpp2

Ikkatai Y., Watanabe S., 2015. Eye surface temperature detects stress response in budgerigars (*Melopsittacus undulatus*). Neuroreport 26(11): 642–646. doi:10.1097/WNR.0000000000000403

James D., Hornik K., 2022. `chron`: Chronological Objects which Can Handle Dates and Times. R package version 2.3-57. S original by David James, R port by Kurt Hornik. Available at: https://CRAN.R-project.org/package=chron

Jerem P., Herborn K., McCafferty D., McKeegan D., Nager R. 2015. Thermal imaging to study stress non-invasively in unrestrained birds. J. Vis. Exp. 2015(105): 1–10. doi:10.3791/53184

Jerem P., Jenni-Eiermann S., McKeegan D., McCafferty D.J., Nager R.G., 2019. Eye region surface temperature dynamics during acute stress relate to baseline glucocorticoids independently of environmental conditions. Physiol. Behav. 210: 112627. doi:10.1016/j.physbeh.2019.112627

Kryštufek B., Vohralík V., 2009. Mammals of Turkey and Cyprus. Rodentia II: Cricetinae, Muridae, Spalacidae, Calomyscidae, Capromyidae, Hystricidae, Castoridae. Univerza na Primorskem, Znanstveno-raziskovalno središčě, Zalozba Annales: Zgodovinsko drusťvo za juzňo Primorsko, University of Primorska, Science and Research Centre Koper, Garibaldijeva 1, 6000 Koper, Slovenia.

Langford D.J., Bailey A.L., Chanda M.L., Clarke S.E., Drummond T.E., Echols S., Glick S., Ingrao J., Klassen-Ross T., Lacroix-Fralish M.L., Matsumiya L., Sorge R.E., Sotocinal S.G., Tabaka J.M., Wong D., Van Den Maagdenberg A.M.J.M., Ferrari M.D., Craig K.D., Mogil J.S., 2010. Coding of facial expressions of pain in the laboratory mouse. Nat. Methods 7(6): 447–449. doi:10.1038/nmeth.1455

Lees A.M., Salvin H.E., Colditz I.G., Lee C., 2020. The influence of temperament on body temperature response to handling in angus cattle. Animals 10(1): 1–16. doi:10.3390/ani10010172

Lewden A., Nord A., Petit M., Vézina F., 2017. Body temperature responses to handling stress in wintering Black-capped Chickadees (*Poecile atricapillus* L.). Physiol. Behav. 179: 49–54. doi:10.1016/j.physbeh.2017.05.024

Long N.C., Vander A.J., Kluger M.J., 1990. Stress-induced rise of body temperature in rats is the same in warm and cool environments. Physiol. Behav. 47(4): 773–775. doi:10.1016/0031-9384(90)90093-J

Lucas M., Ilin Y., Anunu R., Kehat O., Xu L., Desmedt A., Richter-Levin G., 2014. Long-term effects of controllability or the lack of it on coping abilities and stress resilience in the rat. Stress 17(5): 423–430. doi:10.3109/10253890.2014.930430

Mason G., 2006. Stereotypic behaviour in captive animals: Fundamentals and implications for welfare and beyond. Stereotypic Anim. Behav. Fundam. Appl. to Welf. Second Ed.: 326–356. doi:10.1079/9780851990040.0325

Mazur-Milecka M., 2016. Thermal imaging in automatic rodent's social behaviour analysis. In: 13th International Conference on Quantitative Infrared Thermography, January 2016.

McCafferty D.J., 2007. The value of infrared thermography for research on mammals: Previous applications and future directions. Mamm. Rev. 37(3): 207–223. doi:10.1111/j.1365-2907.2007.00111.x

McCafferty D.J., Gallon S., Nord A., 2015. Challenges of measuring body temperatures of free-ranging birds and mammals. Anim. Biotelemetry 3(1): 1–10. doi:10.1186/s40317-015-0075-2

McGivern R.F., Zuloaga D.G., Handa R.J., 2009. Sex differences in stress-induced hyperthermia in rats: Restraint versus confinement. Physiol. Behav. 98(4): 416–420. doi:10.1016/j.physbeh.2009.07.004

McLeod A.I., Zhang Y., 2008. Improved subset autoregression: With R package. J. Stat. Softw. 28(2): 1-28. doi:10.18637/jss.v028.i02

Minkina W., Dudzik S., 2009. Algorithm of Infrared Camera Measurement Processing Path. Infrared Thermography. John Wiley & Sons, Ltd, Chichester, UK. 41–60.

Mohammed M., Kulasekara K., De Menezes R.C., Ootsuka Y., Blessing W.W., 2013. Inactivation of neuronal function in the amygdaloid region reduces tail artery blood flow alerting responses in conscious rats. Neuroscience 228(June 2017): 13–22. doi:10.1016/j.neuroscience.2012.10.008

Mohammed M., Ootsuka Y., Blessing W., 2014. Brown adipose tissue thermogenesis contributes to emotional hyperthermia in a resident rat suddenly confronted with an intruder rat. Am. J. Physiol. – Regul. Integr. Comp. Physiol. 306(6): 394–400. doi:10.1152/ajpregu.00475.2013

Møller A.P., 2010. Body temperature and fever in a free-living bird. Comp. Biochem. Physiol. – B Biochem. Mol. Biol. 156(1): 68–74. doi:10.1016/j.cbpb.2010.02.006

Möstl E., Rettenbacher S., Palme R., 2005. Measurement of corticosterone metabolites in birds' droppings: An analytical approach. Ann. N. Y. Acad. Sci. 1046: 17–34. doi:10.1196/annals.1343.004

Mota-Rojas D., Olmos-Hernández A., Verduzco-Mendoza A., Lecona-Butrón H., Martínez-Burnes J., Mora-Medina P., Gómez-Prado J., Orihuela A., 2021. Infrared thermal imaging associated with pain in laboratory animals. Exp. Anim. 70(1): 1–12. doi:10.1538/EXPANIM.20-0052

Müller M., 2007. Dynamic Time Warping. Information Retrieval for Music and Motion. Springer Berlin Heidelberg, Berlin, Heidelberg. 69–84.

Nakamori T., Morimoto A., Morimoto K., Tan N., Murakami N., 1993. Effects of α- and β-adrenergic antagonists on rise in body temperature induced by psychological stress in rats. Am. J. Physiol. – Regul. Integr. Comp. Physiol. 264(1): R156–R161. doi:10.1152/ajpregu.1993.264.1.r156

Nakamura K., 2015. Neural circuit for psychological stress-induced hyperthermia. Temperature 2(3): 352–361. doi:10.1080/23328940.2015.1070944

Navarro-Castilla Á., Barja I., 2014. Does predation risk, through moon phase and predator cues, modulate food intake, antipredatory and physiological responses in wood mice (*Apodemus sylvaticus*)? Behav. Ecol. Sociobiol. 68(9): 1505–1512. doi:10.1007/s00265-014-1759-y

Navarro-Castilla Á., Barja I., 2019. Stressful living in lower-quality habitats? Body mass, feeding behavior and physiological stress levels in wild wood mouse populations. Integr. Zool. 14(1): 114–126. doi:10.1111/1749-4877.12351

Navarro-Castilla Á., Diaz M., Barja I., 2017. Does ungulate disturbance mediate behavioural and physiological stress responses in Algerian mice (*Mus spretus*)? a wild exclosure experiment. Hystrix 28(2): 165–172. doi:10.4404/hystrix-28.2-12332

Nord A., Folkow L.P., 2019. Ambient temperature effects on stress-induced hyperthermia in Svalbard ptarmigan. Biol. Open 8(6): 1–5. doi:10.1242/bio.043497

Oka T., Kanemitsu Y., Sudo N., Hayashi H., Oka K., 2013. Psychological stress contributed to the development of low-grade fever in a patient with chronic fatigue syndrome: A case report. Biopsychosoc. Med. 7(1): 1–7. doi:10.1186/1751-0759-7-7

Olivas I., Villagrá A., 2013. Effect of handling on stress-induced hyperthermia in adult rabbits. World Rabbit Sci. 21(1): 41–44. doi:10.4995/wrs.2013.1178

Olivier B., 2015. Psychogenic fever, functional fever, or psychogenic hyperthermia? Temperature 2(3): 324–325. doi:10.1080/23328940.2015.1071701

Palme R., 2005. Measuring fecal steroids: Guidelines for practical application. Ann. N. Y. Acad. Sci. 1046: 75–80. doi:10.1196/annals.1343.007

Palme R., 2019. Non-invasive measurement of glucocorticoids: Advances and problems. Physiol. Behav. 199: 229–243. doi:10.1016/J.PHYSBEH.2018.11.021

Peloso E., Wachulec M., Satinoff E., 2002. Stress-induced hyperthermia depends on both time of day and light condition. J. Biol. Rhythms 17(2): 164–170. doi:10.1177/074873002129002456

Phillips P.K., Heath J.E., 1995. Dependency of surface temperature regulation on body size in terrestrial mammals. J. Therm. Biol. 20(3): 281–289. doi:10.1016/0306-4565(94)00061-M

R Core Team. 2021. R: A language and environment for statistical computing. R Foundation for Statistical Computing. R Core Team, 2021.09.0. Vienna, Austria. Available at: https://www.R-project.org/

Rasmussen S., Miller M.M., Filipski S.B., Tolwani R.J., 2011. Cage change influences serum corticosterone and anxiety-like behaviors in the mouse. J. Am. Assoc. Lab. Anim. Sci. 50(4): 479–483.

Romero L.M., 2004. Physiological stress in ecology: Lessons from biomedical research. Trends in Ecology and Evolution, Elsevier Current Trends. 249–255.

Rorick-Kehn L.M., Hart J.C., McKinzie D.L., 2005. Pharmacological characterization of stress-induced hyperthermia in DBA/2 mice using metabotropic and ionotropic glutamate receptor ligands. Psychopharmacology (Berl). 183(2): 226–240. doi:10.1007/s00213-005-0169-2

Sanger M.E., Doyle R.E., Hinch G.N., Lee C., 2011. Sheep exhibit a positive judgement bias and stress-induced hyperthermia following shearing. Appl. Anim. Behav. Sci. 131(3–4): 94–103. doi:10.1016/j.applanim.2011.02.001

Sapolsky R.M., Romero L.M., Munck A.U., 2000. How do glucocorticoids influence stress responses? Integrating permissive, suppressive, stimulatory, and preparative actions. Endocr. Rev. 21(1): 55–89. doi:10.1210/er.21.1.55

Schaefer A.L., Cook N.J., Bench C., Chabot J.B., Colyn J., Liu T., Okine E.K., Stewart M., Webster J.R., 2012. The non-invasive and automated detection of bovine respiratory disease onset in receiver calves using infrared thermography. Res. Vet. Sci. 93(2): 928–935. doi:10.1016/j.rvsc.2011.09.021

Schmelting B., Corbach-Söhle S., Kohlhause S., Schlumbohm C., Flügge G., Fuchs E., 2014. Agomelatine in the tree shrew model of depression: Effects on stress-induced nocturnal hyperthermia and hormonal status. Eur. Neuropsychopharmacol. 24(3): 437–447. doi:10.1016/j.euroneuro.2013.07.010

Senin, P., 2008. Dynamic time warping algorithm review. Information and Computer Science Department University of Hawaii at Manoa Honolulu, USA. 855(1–23): 40.

Sikes R.S., Gannon W.L., 2011. Guidelines of the American Society of Mammalogists for the use of wild mammals in research. J. Mammal. 92(1): 235–253. doi:10.1644/10-MAMM-F-355.1

Smith S.M., Vale W.W., 2006. The role of the hypothalamic-pituitary-adrenal axis in neuroendocrine responses to stress. Dialogues Clin. Neurosci. 8(4): 383–395. doi:10.31887/dcns.2006.8.4/ssmith

Steimer T., 2011. Animal models of anxiety disorders in rats and mice: Some conceptual issues. Dialogues Clin. Neurosci. 13(4): 495–506. doi:10.31887/dcns.2011.13.4/tsteimer

Stewart M., Stookey J.M., Stafford K.J., Tucker C.B., Rogers A.R., Dowling S.K., Verkerk G.A., Schaefer A.L., Webster J.R., 2009. Effects of local anesthetic and a nonsteroidal antiinflammatory drug on pain responses of dairy calves to hot-iron dehorning. J. Dairy Sci. 92(4): 1512–1519. doi:10.3168/jds.2008-1578

Stewart M., Verkerk G.A., Stafford K.J., Schaefer A.L., Webster J.R., 2010. Noninvasive assessment of autonomic activity for evaluation of pain in calves, using surgical castration as a model. J. Dairy Sci. 93(8): 3602–3609. doi:10.3168/jds.2010-3114

Stewart M., Webster J.R., Schaefer A.L., Cook N.J., Scott S.L., 2005. Infrared thermography as a non-invasive tool to study animal welfare. Anim. Welf. 14(4): 319–325.

Stewart M., Webster J.R., Verkerk G.A., Schaefer A.L., Colyn J.J., Stafford K.J., 2007. Non-invasive measurement of stress in dairy cows using infrared thermography. Physiol. Behav. 92(3): 520–525. doi:10.1016/j.physbeh.2007.04.034

Still C., Powell R., Aubrecht D., Kim Y., Helliker B., Roberts D., Richardson A.D., Goulden M., 2019. Thermal imaging in plant and ecosystem ecology: applications and challenges. Ecosphere 10(6): e02768. doi:10.1002/ecs2.2768

Šumbera R., Zelová J., Kunc P., Knížková I., Burda H., 2007. Patterns of surface temperatures in two mole-rats (Bathyergidae) with different social systems as revealed by IR-thermography. Physiol. Behav. 92(3): 526–532. doi:10.1016/j.physbeh.2007.04.029

Tattersall G.J., 2016. Infrared thermography: A non-invasive window into thermal physiology. Comparative Biochemistry and Physiology – Part A: Molecular and Integrative Physiology, Elsevier Inc. 78–98.

Tattersall G.J., Cadena V., 2010. Insights into animal temperature adaptations revealed through thermal imaging. Imaging Sci. J. 58(5): 261–268. doi:10.1179/136821910X12695060594165

Thierry A.M., Ropert-Coudert Y., Raclot T., 2013. Elevated corticosterone levels decrease reproductive output of chick-rearing Adélie penguins but do not affect chick mass at fledging. Conserv. Physiol. 1(1): 1–12. doi:10.1093/conphys/cot007

Tranquillo C., Villa F., Wauters L.A., Dantzer B., Palme R., Preatoni D., Martinoli A., Santicchia F., 2022. Physiological stress and spatio-temporal fluctuations of food abundance and population density in Eurasian red squirrels. Hystrix 33(1) (online first) doi:10.4404/hystrix-00493-2021

Trapletti A., Hornik K., 2019. Package `tseries`: time series analysis and computational finance. R package version 0.10-47. Available at: https://CRAN.R-project.org/package=tseries

Travain T., Valsecchi P., 2021. Infrared thermography in the study of animals' emotional responses: A critical review. Animals 11(9). 2510. doi:10.3390/ani11092510

Van Der Heyden J.A.M., Zethof T.J.J., Olivier B., 1997. Stress-induced hyperthermia in singly housed mice. Physiol. Behav. 62(3): 463–470. doi:10.1016/S0031-9384(97)00157-1

Vogel B., Wagner H., Gmoser J., Wörner A., Löschberger A., Peters L., Frey A., Hofmann U., Frantz S. 2016. Touch-free measurement of body temperature using close-up thermography of the ocular surface. MethodsX 3: 407–416. doi:10.1016/j.mex.2016.05.002

Wickham H., 2009. Elegant Graphics for Data Analysis: `ggplot2`. Springer, New York.

Yang W., Zhou X., Ma T., 2019. Memory Decline and Behavioral Inflexibility in Aged Mice Are Correlated With Dysregulation of Protein Synthesis Capacity. Front. Aging Neurosci. 11(September): 1–9. doi:10.3389/fnagi.2019.00246

Associate Editor: L.A. Wauters

Supplemental information

Additional Supplemental Information may be found in the online version of this article:

Table S1 Descriptive statistics of T_{max} for different subsets of the data

Table S2 Parameter estimates for SARIMA models

Figure S3 Residual check for the all captures model (0,0,1)(0,1,0)[103]

Figure S4 Residual check for final models

Figure S5 Mapping of the stationary sequences "First Captures" and "1st Recaptures"

Figure S6 Mapping of the stationary sequences "First Captures" and "2nd Recaptures"

Figure S7 Mapping of the stationary sequences "First Captures" and "3rd Recaptures"